Detecting Sensor Failures in TDOA-based Passive Radars: A Statistical Approach based on Outlier Distribution

Gaetano Giunta, *IEEE Senior Member*, Luca Pallotta, *IEEE Senior Member*, and Danilo Orlando, *IEEE Senior Member*

***Abstract*—Non-cooperative target location is accomplished by means of multiple passive radar receivers deployed in the region of interest and that detect the delayed replicas of the signal emitted by the target and estimate the time difference of arrival. However, in realistic scenarios, some of the involved sensors could not correctly work if the sensor is victim of intentional/unintentional interference and/or physical damage of the device or its communication link. Thus, procedures for failure detection become of primary interest to discard the measurements related to the out-of-order sensors. The approach proposed in this paper identifies sensors under failure from the analysis of the errors in the equation system implemented to estimate the delays. More precisely, we first compute the second and fourth order correlations (namely, cross-correlation and cross-cross-correlation, i.e. the cross-correlation between signals' cross-correlations) of the incoming signals to build up the system of equation. Then, we perform a sequential cancellation of the equations that experience the highest errors. A statistical test based on the number of canceled equations related to a specific sensor is used to state whether or not the specific sensor is under failure. Finally, the performance of the entire failure detection architecture is assessed by numerical simulations also in comparison with a heuristic method based on the percentages of canceled equations and its standard counterparts not performing any outlier screening.**

***Index Terms*—Delay estimation, outlier cancellation, sensor failure, cross-correlation, time difference of arrivals, passive/green radar.**

I. Introduction

TIME difference of arrival (TDOA) is often exploited by the emerging green/passive radar technology for non-cooperative target positioning [1]–[5]. This is done by interpolating the TDOA measurements associated with the replicas of the radar/communication signals emitted by the target and intercepted by a set of receiving sensors. The time of arrivals used in the localization process are obtained by estimating the time instants where the peaks of the cross-correlation (CC) between the incoming signal and a reference one lie [6]–[8]. To improve the estimation accuracy, the generalized cross-correlation (GCC) [6] applies a filter to the replicas computing the cross-correlations. The main drawback of the GCC is that it has a low practical value since it requires prior information about the signal and noise spectral properties. In fact, the GCC is based on the ideal assumption of a perfect a-priori knowledge of the signal and noise spectra used to prefilter the incoming signal. This operation is applied to the signal cross-correlation and then such a filtered cross-correlation exploited to estimate the signal delay. In the case of non-cooperative targets, the assumption required by the GCC is no longer valid and, hence, it is not possible to filter the cross-correlation. As a consequence, GCC might experience a severe performance degradation [8]. This limitation is overcome in [8] where a delay estimation method, that intrinsically implements the GCC filter without prior information, is designed. Such a method goes beyond the classic cross-correlation and exploits a particular fourth-order correlation between sensor signals, namely the cross-cross-correlation (CCC), i.e., the cross-correlation of each pair of cross-correlations of the received signals, to improve the estimation accuracy. In fact, such a method leads to an increment of the equations involved in the estimation process.

The main drawback of the aforementioned methods arises in realistic scenarios, where some measurements could be affected by outliers, leading to a possible performance degradation or even to a nonworking condition of the sensor. A sensor failure might occur when it is affected by intentional and/or unintentional interference or physical damages of the device or its communication link. Generally speaking, several strategies have been developed over the years to cope with the problem of outliers identification in TDOA-based localization [9]–[14]. However, it would be indispensable to guarantee the correct functioning of the entire system, not only by removing outliers from measurements, but also by establishing if one or more sensors are under failure. Therefore, in such a situation, it is important to implement procedures aimed at identifying failure conditions in order to excise all the measurements acquired by the damaged sensors.

With the above remarks in mind, this paper proposes the design of a methodology for the identification of sensors' failure in the context of passive radars. In particular, the method consists of a two-stage algorithm, where in the first stage the outliers are identified and in the second stage a statistical procedure to decide for a sensor failure is applied. In more detail, starting from the measurements of signal's replicas, at the first stage, several cross-correlations and/or cross-cross-correlations of the incoming signals are computed. These moments are used to form an equation system whose solutions are the delay

G. Giunta and L. Pallotta (*corresponding author*) are with Industrial, Electronic and Mechanical Engineering Department, University of Roma Tre, via Vito Volterra 62, 00146 Rome, Italy. E-mail: gaetano.giunta@uniroma3.it, luca.pallotta@uniroma3.it

D. Orlando is with Università degli Studi "Niccolò Cusano", Via Don Carlo Gnocchi 3, 00166 Roma, Italy. E-mail: danilo.orlando@unicusano.it.

estimates. Then, a sequential procedure for outlier detection and cancellation based on the highest values of the mean square error (MSE) is invoked. Once the outlier equations are canceled, the method stores the number of excised equations in which each sensor was involved (these numbers are considered warning scores). The second stage of the algorithm is then a statistical test based on the assumed distribution of the warning scores associated with each deployed sensor. Once a sensor failure is detected, all the equations related to it are removed from the entire overdetermined system (in fact, inhibiting the functioning of the specific sensor) and the final delay estimates are derived from the resulting reduced-size system. Numerical simulations are conducted to demonstrate the effectiveness of the proposed method also in comparison with a heuristic approach that makes use of the percentages of canceled equations to set the detection threshold. Finally, the root mean square error (RMSE) of the estimated delays is used to assess the performance of the whole method in both scenarios with and without sensor failures, showing its gains over standard counterparts not performing any outlier screening.

The reminder of the paper is organized as follows. In Section II the formal statement of the estimation problem is provided for both CC and CCC-based methods. Section III describes the proposed algorithm including the statistical method for failure detection. Section IV shows and discusses some illustrative examples. Finally, Section V concludes the manuscript and draws some hints for possible future research lines.

II. Delay Estimation in Passive Radar with Multiple Receivers

For the reader's convenience, in this section we briefly review some recent location methods using passive networks [8] whose robustness to sensor failure is enhanced through the strategy devised in Section III.

A passive location system estimates the target position by processing suitable measurements related to the target signal and collected by $M > 2$ noncolocated sensors. This scenario is illustrated in Figure 1, where multiple sensors are used to localize a target. Moreover, the picture also shows a possible status of failure that could occur for one or more sensors.

Assuming an anechoic scenario, the signal received at the i-th detection node, $r_i(\cdot) \in \mathbb{C}$, and sampled at time instants nT, with $n \in \mathbb{N}$ and T the sampling period, can be described as[1]

$$r_i(nT) = \gamma_i s(nT - t_i) + w_i(nT), \quad i = 0, \ldots, M-1, \quad (1)$$

[1]The proposed signal model does not account for the Doppler component that could be also included, therefore, generalizing the cross-correlation to the cross-ambiguity function. However, it is worth observing that, in practice, for short-time observation intervals, the Doppler component can be neglected especially when the bandwidth of the receiver is much greater than the Doppler shifts generated by the non-cooperative target. Conversely, in the presence of narrowband radars or if much more data are employed for integration, some preliminary procedure for Doppler compensation is required before the application of any algorithm for time delay estimation.

where t_i is the unknown delay at receiver i, $s(\cdot) \in \mathbb{C}$ is the unknown signal transmitted by the target, $\gamma_i \in \mathbb{C}$ is a scaling factor accounting for propagation effects between the target and the i-th node as well as the transmitted power, and $w_i(\cdot) \in \mathbb{C}$ is the noise contribution at the i-th sensing node that is assumed to be uncorrelated with $s(\cdot)$.

It is important to observe that as in [8], the considered framework assumes that the receivers are synchronized in the time and frequency domain. However, in practice, the effects related to time and/or frequency synchronization errors should be accounted for. To this end, notice that the time synchronization error can be mitigated by resorting to GPS signals or a common synchronization signal transmitted over a wired connection. Moreover, as to the frequency synchronization it is worth observing that, since each receiver uses its own local oscillator, the oscillator frequencies can be different from each other. Now, two issues could arise: 1) how ensuring the same initial phase, 2) how maintaining the same oscillation frequency for downconversion. The first issue can be solved sending a temporal pilot synchronization signal, whereas the second can be addressed through one of the following strategies: a) one receiver estimates the centroid of the spectrum, after Doppler compensation, and then shares this value with the other receivers; b) each receiver compensates the Doppler and performs the centroid estimation by itself (see also footnote 1). The TDOA estimation problem of the signals measured by the M sensors can be written in terms of the following matrix equation [8]

$$\boldsymbol{X} \begin{bmatrix} t_1 \\ \vdots \\ t_{M-1} \end{bmatrix} = \begin{bmatrix} \hat{b}_1 \\ \vdots \\ \hat{b}_Q \end{bmatrix}, \quad (2)$$

where $\hat{b}_1, \ldots, \hat{b}_Q$ are Q measurements with $Q > M$ derived from the position of the maximum in the magnitude of all the possible correlations between the M signals, including the classical second-order CC and (optionally) the fourth-order CCC recently introduced in [8]. Moreover, $\boldsymbol{X} \in \mathbb{R}^{Q \times (M-1)}$ is a sparse matrix that assumes nonzero elements according to the indices of the signals involved in each correlation. The number of rows Q depends on which algorithm is used

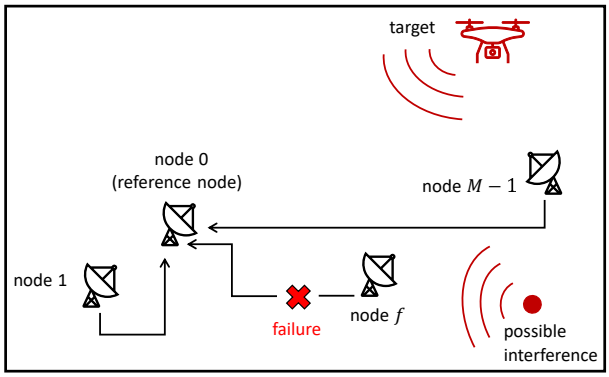

Figure 1: Graphical illustration of a passive/green radar working principle.

among CC, CCC, or even both of them (say CCC2) [8]. The overdetermined system (2) can be solved resorting to the least squares (LS) approach.

Finally, it is worth highlighting that, in scenarios of practical interest, some measurements might be impaired by hardware/software anomalous behavior, environment interference, or intentional attacks. In such cases, LS-based approaches tend to experience a performance degradation since they return a suboptimal solution that does not account for possible outliers in the measurements. In order to face these situations, anomalous estimates can be detected and the corresponding measurements can be discarded from the available data. Moreover, the sensor responsible for these discarded measurements can be disabled and declared to be in failure state.

With the above remarks in mind, in the next section, an algorithm aimed at increasing the robustness of the CC/CCC/CCC2 in the presence of outliers and/or sensor failures is devised.

III. Proposed Algorithm

The proposed framework is based on the idea of excising those equations affected by anomalies by marking them as *outliers* in the overall set of equations. Every equation derives from correlations between a subset of sensors, and when classified as outlier, it can give a hint (i.e., a *warning*) of possible failure of the sensors associated with that equation. In the absence of sensor failures, the erroneous equations (likely due to noise effect) produce randomly distributed outliers, so that the *warning scores* (i.e., the sum of all ascribed warnings) among the sensors are expected to be statistically uniform. Conversely, sensor failure should cause a higher peak in the warning score of the faulty sensor. Therefore, testing for the warning score can result in an effective metric to detect failure situations even under noisy scenarios.

To this end, the warning score of each sensor is the number of equations identified as *outlier equations* (at the previous step) selected from a set of equations associated with the sensor under consideration. Once the warning scores are computed, the algorithm makes a test on the number of warning scores to decide for a possible sensor failure. In order to improve TDOA estimation performance, the equations identified as outliers or associated with sensors under failure can be finally canceled in the original overdetermined system.

The block scheme of the proposed methodology is depicted in Figure 2. This scheme can be applied considering one of the aforementioned CC, CCC, and CCC2 algorithms. The algorithm starts with the acquisition of the measurements from each receiving sensor node, $r_i(nT)$, $i = 0, \dots, M-1$. After signals acquisition their respective cross- and cross-cross-correlations are computed. These are then gathered together to construct the system of equations from which the delay estimates can be obtained. Once the system of equations is formed, it could happen that some of them significantly differ (in the sense of their high delay estimation errors) from the others. This can be due to for instance:

- intentional interference (e.g., noise jamming) aimed at inhibiting the functionality of the locating system,
- unintentional disturbance (such as noise spikes as well as other communication systems working in the same frequency band),
- malfunction of one or more sensors/communication links (e.g., hardware failure or synchronization problems), as well as Non Line-Of-Sight (NLOS) propagation.

Therefore, the method, after solving the CC/CCC/CCC2 problem, provides the conventional delays estimates together with the errors associated with each equation. Then, the equations sharing the higher errors are removed before computing a new solution of the reduced-size system of equations. In particular, the proposed architecture is based on a first weak outlier equations cancellation followed by a strong outlier equations cancellation (more details about the equation cancellation procedure are given in Section III-A). Once the cancellation of the outlier equations is performed, the detection of a failed sensor is accomplished (see Subsection III-B). Then, if a sensor is detected to be under failure, all the measurements coming from it are rejected. This is done removing all the equations in which that sensor is involved and the final reduced-size CC/CCC/CCC2 problem is solved providing the robust delay estimates.

Additionally, for the sake of comparison, a heuristic threshold setting method for the warning score is also described in Subsection III-C. More precisely, a sensor failure is declared if the warning score exceeds a parametric pre-fixed quota (independent of the score distribution) of the total number of equations of the original system in which the specific sensor is involved.

In all cases, in the presence of sensor failure declaration, the estimated delays $\hat{t}_i$ only belong to a set indexing correctly working sensors, namely, $\hat{t}_i \notin \Omega_f$, with $\Omega_f = f_1, f_2, \dots$ the set of indices of sensors under failure. On the other hand, if no sensor is declared under failure, only the measurements of those equations labeled to be outliers are rejected. The entire procedure is summarized in Algorithm 1, with reference to CC, CCC, and CCC2.

Algorithm 1 Procedure for robust delay estimation in the presence of possible sensor failure.

Input: Received signals at each sensor r_i, $i = 0, \dots, M-1$.
Output: Estimated time delays $\hat{t}_i$, with $i \notin \Omega_f$, set of failed sensors Ω_f.

1: Construct the model matrix and the measurements vector from the peaks' positions of the cross- and/or cross-cross-correlations;
2: Solve CC/CCC/CCC2 problem;
3: Compute equations errors;
4: Identification and cancellation of the outlier equations from the system of equations through Algorithm 2;
5: Identification of the failed sensors through Algorithm 3;
6: **if** Failures are declared **then**
7: Cancellation of all the equations related to the identified failed sensors;
8: **end if**
9: Solve the possibly reduced CC/CCC/CCC2 problem.

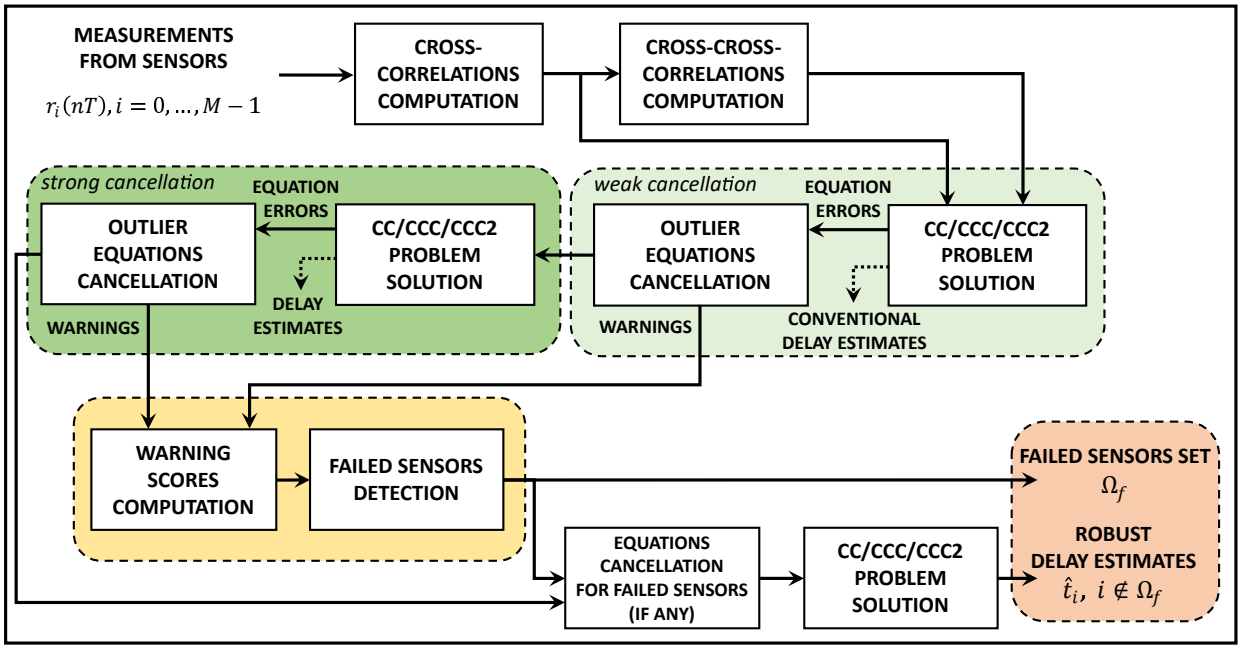

Figure 2: Block scheme of the proposed robust method for delays estimation under sensor failure conditions.

A. Outliers cancellation procedure

The considered procedure for outliers rejection in the CC/CCC/CCC2 problem basically performs the evaluation of the absolute error associated with the estimated delay vector $\boldsymbol{t}$. In particular, the equations exhibiting the higher values of the absolute error are rejected leading to a new smaller system of more accurate equations. With reference to the CC/CCC/CCC2, the absolute errors are defined as

$$\boldsymbol{e} = [e_1, \ldots, e_Q]^T = |\boldsymbol{X}\hat{\boldsymbol{t}} - \boldsymbol{b}|, \tag{3}$$

where Q is the overall number of equations and it is equal to $\left(M^2 - M\right)/2$ (for CC), $(1/4)M^4 - (1/2)M^3 - (1/4)M^2 + (1/2)M$ (for CCC), and $(1/4)M^4 - (1/2)M^3 + (1/4)M^2$ (for CCC2) [8]. Moreover, $\boldsymbol{b}$ is the measurements vector described in the right-hand side of the LS equations described in [8]. Finally, $\hat{\boldsymbol{t}}$ is the vector containing the estimates of the delays $t_1 \ldots, t_{M-1}$, and $|\cdot|$ denotes the absolute value of each element of the vector argument.

Each entry of $\boldsymbol{e}$ is then used as decision statistic for outliers identification. Precisely, each value e_q is compared with a specific threshold η to decide between two alternative hypotheses, viz. H_1 (presence of outlier) vs H_0 (absence of outlier). Once the tests are performed, the equations in the LS problem for which $e_q > \eta$ are canceled getting a new reduced-size LS problem. As to the threshold η, it is set equal to the median absolute deviation (MAD)[2] [15], [16], that is

$$\eta = \kappa\mu\,\text{median}\left(|\boldsymbol{e} - \text{median}(\boldsymbol{e})|\right), \tag{4}$$

where median$(\cdot)$ is the median value of its arguments, $\mu = 1.4826$ is a constant value detailed in [15], [16].[3] Moreover, κ is a parameter typically chosen between 2 and 3 that allows to a-priori establish the deepness of outliers excision [15], [16]. In fact, it plays the role of a tuning parameter which manages the trade-off between the amount of outliers cancellation and the overall estimation accuracy. More precisely, a low value of κ (e.g., 2) implies a strong cancellation with a high number of excised equations, meanwhile a large value of κ (e.g., 3) allows the algorithm to delete only the reduced number of the 'wrongest' equations. As shown also in [17], these remarks lay the groundwork for a sequential cancellation to gradually refine the tuning parameter κ starting from a high value so as the 'wrong' equations are little by little identified as outliers and hence removed. With reference to the proposed framework, κ starts from the value 3 (weak cancellation in Figure 2), and at the next step is reduced to the value 2 (strong cancellation in Figure 2). The step size in passing from $\kappa = 3$ to $\kappa = 2$ is set according to practical aspects such as the total number of equations and computational requirements (also ensured to be limited because of the closed-form and offline evaluation of the pseudo-inverse solution). For the reader's convenience, the pseudo-code of the outliers cancellation procedure is given in Algorithm 2.

[2]The MAD outlier detection model is used, for non-Gaussian data, for its higher accuracy and robustness due to its independence to mean and standard deviation [15], [16]. Generally speaking, methods based on the median value are more robust than those exploiting the mean when data move away from gaussianity. Therefore, since we do not have knowledge about the statistical behaviour of the equation errors, a median-based estimator represents the best compromise between robustness and accuracy.

[3]Note that, the value of μ is set equal to 1.4286 in the Literature when data are assumed Gaussian distributed. Then, MAD measures the deviation from gaussianity according with the expression in (4). In this case, data are related to the absolute error, that, cannot be Gaussian distributed. However, we proved different values for μ (not reported for brevity), and the best solution is provided by that value.

Algorithm 2 Outliers cancellation procedure.

Input: Model matrix $\boldsymbol{X}$, measurements vector $\boldsymbol{b}$.
Output: Indices of the equations marked as outliers.

1: **for** $\kappa = 3$ **to** $\kappa = 2$ **do**
2: CC/CCC/CCC2 solution and absolute error computation, $\hat{\boldsymbol{t}}$ and $\boldsymbol{e}$;
3: Threshold computation using the MAD through (4);
4: **if** Equations errors > threshold **then**
5: Identification of outlier equations;
6: Cancellation of the identified outlier equations from the system of equations;
7: **end if**
8: **end for**

B. Proposed statistical method

After the equations are identified as outliers and canceled at stage one, the warning scores to ascribe to the sensors are evaluated as follows. Precisely, one warning is ascribed to a sensor if it is involved in the computation of the cross- or cross-cross-correlation used in the removed equation. Therefore, three different situations could arise:

- the warning is ascribed to 2 sensors because the removed equation considers a cross-correlation (i.e., the rows of (2));
- the warning is ascribed to 3 sensors because the removed equation uses a cross-cross-correlation involving 3 different measurements, when two subscripts in the rows of the LS problem are the same;
- the warning is ascribed to 4 sensors because the removed equation derives from a cross-cross-correlation involving 4 different measurements (rows in the LS problem with four different subscripts).

Then, the warning score for each sensor is evaluated as the sum of all the warnings assigned to it. It is worth observing that, in the absence of sensor failures, it is expected that the warning scores associated with all sensors are close to each others, essentially having almost the same number of canceled equations. Conversely, when a sensor is under a failure condition, its corresponding warning score will be much higher than the others. Let us denote by N_2, N_3, and N_4 the number of outlier equations related to 2, 3, or 4 sensors, respectively. Notice that in the proposed architecture, such numbers can be obtained at the output of the outlier equations cancellation procedure. Under the null hypothesis, we assume a fully-random model for the warning scores, where all the errors are independent of each other and due to random noise only (i.e., without sensor failures). In fact, under H_0 hypothesis the warnings are due to noise and hence can be assumed to be uniformly distributed. Now, we can establish the probability mass function (pmf) of the number of warning scores associated with each specific sensor. To this end, let us observe that the warning scores in the case of cancellation of an equation involving two sensors is a binomial random variable with parameters N_2 and $2/M$, say $x_2 \sim \mathcal{B}(N_2, 2/M)$ whose pmf is given by:

$$P_{x_2}(x; N_2, M) = \binom{N_2}{x} \left(\frac{2}{M}\right)^x \left(1 - \frac{2}{M}\right)^{N_2 - x}, \quad x = 0, 1, \ldots, N_2, \tag{5}$$

being, N_2 the total number of removed equations of type 2 and $2/M$ the probability of a single Bernoulli test, i.e., the probability of selecting one sensor.

Similarly, in the case of cancellation of equations involving 3 or 4 sensors, the number of warning scores is again a binomial random variable, viz. $x_3 \sim \mathcal{B}(N_3, 3/M)$ and $x_4 \sim \mathcal{B}(N_4, 4/M)$, whose pmfs are:

$$P_{x_3}(x; N_3, M) = \binom{N_3}{x} \left(\frac{3}{M}\right)^x \left(1 - \frac{3}{M}\right)^{N_3 - x}, \quad x = 0, 1, \ldots, N_3, \tag{6}$$

and

$$P_{x_4}(x; N_4, M) = \binom{N_4}{x} \left(\frac{4}{M}\right)^x \left(1 - \frac{4}{M}\right)^{N_4 - x} \quad x = 0, 1, \ldots, N_4. \tag{7}$$

Finally, the total number of warning scores for each sensor is given by the sum of the three above, i.e., $\mathrm{x} = x_2 + x_3 + x_4$. Assuming a fully random model for the warning scores, and hence assuming x_2, x_3, and x_4 independent each other, x is a random variable whose pmf is given by the convolution between their pmfs described in (5)-(7), that is

$$\begin{aligned} &P_{\mathrm{x}}(x; N_2, N_3, N_4, M) = \\ &\quad P_{x_2}(x; N_2, M) * P_{x_3}(x; N_3, M) * P_{x_4}(x; N_4, M) = \\ &\quad \sum_{q=0}^{x} \sum_{p=0}^{q} \binom{N_2}{p} \binom{N_3}{q-p} \binom{N_4}{x-q} \left(\frac{2}{M}\right)^p \\ &\quad \times \left(1 - \frac{2}{M}\right)^{N_2 - p} \left(\frac{3}{M}\right)^{q-p} \left(1 - \frac{3}{M}\right)^{N_3 - (q-p)} \\ &\quad \times \left(\frac{4}{M}\right)^{x-q} \left(1 - \frac{4}{M}\right)^{N_4 - (x-q)}, \end{aligned} \tag{8}$$

having indicated with $*$ the discrete convolution operation. Let us note that also the distribution $P_{\mathrm{x}}(x; N_2, N_3, N_4, M)$ depends on the specific values N_2, N_3, and N_4.

Now, for each receiving sensor, the resulting problem can be defined as a binary hypothesis test aimed at discriminating between the absence or presence of a failure, that is,

$$\begin{cases} H_{F,0}: & \text{sensor working} \\ H_{F,1}: & \text{sensor failure} \end{cases} \tag{9}$$

The above binary hypothesis testing problem rejects the null hypothesis by comparing the warning score x for sensor i (say $x^{(i)}$) to a specific significance level α, i.e.,

$$x^{(i)} \underset{H_{F,0}}{\overset{H_{F,1}}{\gtrless}} \alpha, \tag{10}$$

where α is a threshold set under $H_{F,0}$ hypothesis as the desired percentile of false failure detections from the pmf

$P_{\mathrm{x}}(x; N_2, N_3, N_4, M)$ of (8) once the numbers N_2, N_3, and N_4 of canceled equations are given (see Section III-A). Summarizing, it is worth underlining that the test is performed for each sensor.

Notice that the value of α can be set by using (8) to compute a preassigned probability of false failure detection. For completeness, Algorithm 3 synthetically describes the main steps involved in the statistical algorithm for sensor failure detection.

Algorithm 3 Statistical algorithm for sensor failure detection.

Input: Matrix structure of $\boldsymbol{A}/\boldsymbol{B}/\boldsymbol{C}$ and indices of the equations marked as outliers.

Output: Indices of sensors detected as under failure, i.e., the set Ω_f.

1: Counting N_2, N_3, and N_4;
2: Counting warning scores $x^{(i)}$, $i = 0, \ldots, M-1$, for each sensor;
3: Set the threshold α that ensures the desired nominal false failure rate applying (8) particularized to N_2, N_3, and N_4 obtained at step 1;
4: Testing $x^{(i)}$, $i = 0, \ldots, M-1$, for sensor failure, through (10).

C. Heuristic procedure

A possible competitor of the proposed method for the detection of sensor under failure compares the warning score of each sensor with a heuristic threshold. Specifically, it is given by

$$x^{(i)} \underset{<}{\overset{H_{F,1}}{>}} \zeta P, \tag{11}$$
$$H_{F,0}$$

where P is the total number of equations in which the specific sensor is involved and $\zeta \in [0, 1)$ a parametric tuning factor that rules the capability of the algorithm to inhibit the acquisitions from a sensor. The parameter ζ can be a-priori set on the basis of specific knowledge about the operative environment and the characteristics of the incoming signals.

A possible operative choice could consist in setting the threshold so as the number of canceled equations overcomes the number of non-canceled equations for the specific sensor, thus resulting $\zeta = 1/2$. By applying such a majority criterion, a conservative behavior of the system is reasonably ensured with respect to its tendency in rejecting sensors. This choice has been used in the numerical simulations described in the next section.

IV. Numerical results and discussion

In this section the performance of the proposed algorithms are assessed in terms of probability of correct failure detection of the i-th sensor, $P_{CFD}^{(i)}$, defined as

$$P_{CFD}^{(i)} = P\left(x^{(i)} > \alpha \,\middle|\, H_{F,1}\right), \quad i = 0, \ldots, M-1. \tag{12}$$

Beyond the analysis of P_{CFD}, it is also worth noting that the proposed test is derived from assumptions made to provide an analytic criterion to the threshold setting. As a consequence, it is necessary to verify how much the resulting threshold provides a false failure detection close to the nominal one. This is verified by considering as figure of merit the probability of false failure detection for the i-th sensor, $P_{FFD}^{(i)}$, defined as

$$P_{FFD}^{(i)} = P\left(x^{(i)} > \alpha \,\middle|\, H_{F,0}\right), \quad i = 0, \ldots, M-1. \tag{13}$$

Finally, to complement the analyses provided in terms of P_{CFD} and P_{FFD}, the relative frequencies of the number of sensors detected to be under failure (i.e., the number of sensors detected to be in failure divided by the total number of trials) are also considered as performance metric. By doing so, information about the inclination of the system in rejecting correctly working sensors in the presence of one of them under failure is assessed.

Simulations are conducted considering the signal transmitted by the target, $s[n]$, composed by 1000 samples. Since, the proposed method does not make any assumption about the nature of the incoming signals, the most general situation with random Gaussian signals is considered. In fact, in a practical scenario the system does not know neither the intercepted signals come from a radar or communication system nor the signal properties such as bandwidth, waveform, etc. More precisely, the signal is generated as a realization of a zero-mean stationary complex Gaussian random process with unit variance and a Gaussian-shaped auto-correlation function [18]

$$\rho_s(\tau) = \exp\left(-\frac{\tau^2}{\sigma_a^2}\right),$$

with $\sigma_a^2 = 2$ its variance. Then, a replica of $s[n]$ is generated at each of the $M-1$ receiving node characterized by a delay uniformly selected in the interval $[0, 1]$ sec (for convenience, the delay at sensor 0 is maintained equal to 0 sec for all simulations). Moreover, the noise contribution is modelled as a white circularly symmetric complex Gaussian vector with the same variance $\sigma_i^2 = \sigma^2$ for all the M sensors. Then, the signal scaling factor γ_i is set, without loss of generality, equal to 1, hence the SNR level is $1/\sigma^2$. Finally, a failure of a sensor is emulated enforcing its corresponding received replica to have the noise component only. Since closed-form expressions for the performance metrics are not available, we resort to Monte Carlo counting techniques and estimate them over $M_c = 10^3$ or 10^4 independent trials for evaluating $P_{CFD}^{(i)}$ and $P_{FFD}^{(i)}$, respectively.

Before assessing the performance of the proposed method, we analyze the goodness of the model approximation leading to equations (5), (6), and (7). To this end, we compare the histograms of the warning scores x_3 obtained through simulated data with the theoretical pmf (6). Simulations are conducted under the H_0 hypothesis, with no sensors under failure and counting the number of warnings for the sensor number 2. We consider a situation where the number of rejected equations is equal to $N_3 = 22$ and $N_3 = 30$, respectively, for a total of 100 occurrences. The results shown in Figure 3 (and

others conducted for N_2 and N_4 not reported here for brevity) point out that the empirical histograms of the warning scores match with their theoretical pmf, thus confirming the validity of the devised model (at least for the considered simulation parameters).

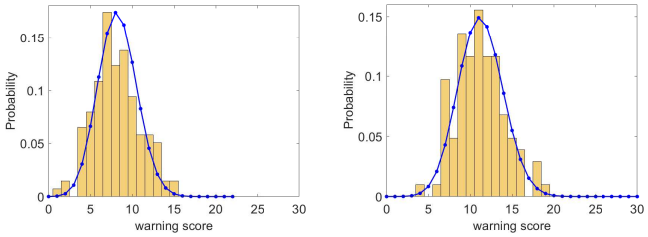

(a) (b)

Figure 3: Theoretical pmf and histogram (evaluated over 100 occurrences) of the warning score x_3. Simulations are conducted considering $M = 8$ sensors, and N_3 equal to a) 22 and b) 30.

The detection performance analysis starts with Figure 4 where the $P_{CFD}^{(i)}$ is plotted as a function of the SNR. More precisely, sensor $i = 2$ is selected to be under failure and a total of $M = 8$ available sensors is considered. The figure compares the proposed statistical sensor failure (SSF) method applied to CC, CCC, and CCC2 (viz. SSF-CC, SSF-CCC, and SSF-CCC2), with respect to the heuristic sensor failure (HSF) based methods (viz. HSF-CC, HSF-CCC, and HSF-CCC2). As to the detection thresholds, for the SSF-based algorithms they are set so as to ensure a nominal probability of false failure detection[4] equal to 10^{-2}, whereas for the HSF-based methods $\zeta = 1/2$ as previously described.[5] As can be seen from the curves, the capability of correctly estimating a failure for the SSF-CCC and SSF-CCC2 is evident. Moreover, also their heuristic counterparts ensure satisfactorily performances for low SNR values, even though a reduced number of sensors (i.e., $M = 8$) is used. However, the detection capabilities of these methods worsen as the SNR increases. This behavior can be explained observing that as the SNR increases, the sub-optimal solution provided by the LS tends to be gradually more accurate (thanks to better estimation of the correlation peaks), which leads to a reduction in the overall number of deleted equations. This latter together with the fact that the heuristic thresholds are fixed, directly reflects in the observed detection losses. Conversely, the SSF-CCC and SSF-CCC2 are capable of maintain the same detection level independently of the SNR, because their thresholds are adaptively set as a function of the number of deleted equations. Finally, the worst estimation appears to be the SSF-CC. This fact can be explained observing that the SSF-CC returns a very low number of equations (e.g., 28 equations for 8 sensors) such that the number of rejected outliers does not differ enough over different sensors. This behavior can be reduced increasing the number of available sensors that in turn results in an increment of the overall number of equations.

The sensitivity analysis for the probability of false failure detection is shown in Figure 5, where $P_{FFD}^{(i)}$ for the sensor $i = 2$ (that is the same as in the correct detection probability analysis) is shown versus SNR for the same scenario as Figure 4, except for the fact that no sensors are under failure. The aim of this analysis is to show that the nominal probability of false alarm is insensitive to the variation of the operating parameter values. This property is important from an operating point of view since the detection threshold can be set using a given set of parameter values and applied in scenarios characterized by different parameter values without altering the nominal probability of false alarm. As expected SSF-CCC and SSF-CCC2 experience a false alarm probability on the specific sensor around the 1%, that is in line with its theoretical value (i.e., 10^{-2}). However, the residual variations around the 1% of the probability of false failure detection (especially for SNR $= 0$ dB) can be explained observing that the decision variable, i.e., the warning score x, is an integer variable, therefore the threshold computed from the pmf is intrinsically quantized (i.e., it is rounded to the highest interest below that value). This produces an integer threshold lower that the one exactly ensuring the desired probability of false failure detection. As a consequence, this reduction in the threshold results in an increment of the current false alarm rate. Additionally, the model devised in (8) derives from considerations that do not exactly match with the realistic situation but that are needed to have an analytic criterion for the threshold estimation. It is also worth observing that for low values of N_2, the threshold can never be reached. In fact, for $M = 8$ and $N_2 = 0, 1, 2, 3$, the threshold is $0, 1, 2$ and 3, respectively, that is the limit for the warning score values related to the specific values of N_2. This has a direct consequence on the actual false alarm of the SSF-CC (see Figure 5), where low values of N_2 are quite frequent. Finally, the figure also reveals that the HSF-CCC and HSF-CCC2 have very low P_{FFD} values, which correspond to lower detection performance as shown in Figure 4.

Figure 6 shows the relative frequencies (expressed in percentage) of the number of sensors detected to be under failure. The simulation setting is the same as in Figure 4. It can be clearly observed that the proposed SSF-CCC and SSF-CCC2 almost always declare only one sensor to be under failure. Moreover, from the comparison with Figure 4 it can be also claimed that it is the true failed sensor. Conversely, as expected form the detection studies, their heuristic counterparts, i.e., HSF-CCC and HSF-CCC2, show some missed detections that increase as the SNR increases because of a lower number of cancelled equations associated with fixed thresholds. Finally, the worst situations are those associated with the SSF-CC and HSF-CC. In fact, SSF-CC has a high number of missed detections, while HSF-CC shows a non-negligible number of detections associated with two sensors as well as a certain amount of missed detections. However, even though detecting

[4]Note that, the theoretical threshold is set at each Monte Carlo trial following the procedure described in Algorithm 3, depending on the values of N_2, N_3, and N_4 obtained as output of the first equations cancellation stage.

[5]Additional numerical results not reported here for brevity have highlighted that $\zeta = 1/2$ represents a good compromise between the number of available sensors and the number of discarded sensors. Moreover, it ensures a reliable performance for the heuristic competitors.

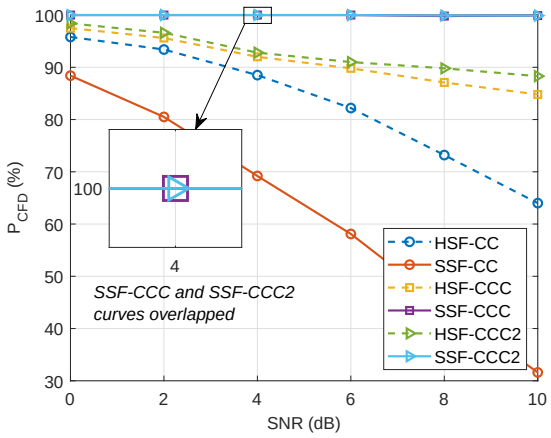

Figure 4: Probability of correct failure detection (%) for sensor 2 versus SNR. The passive radar comprises $M = 8$ sensors, with sensor number 2 set to be under failure.

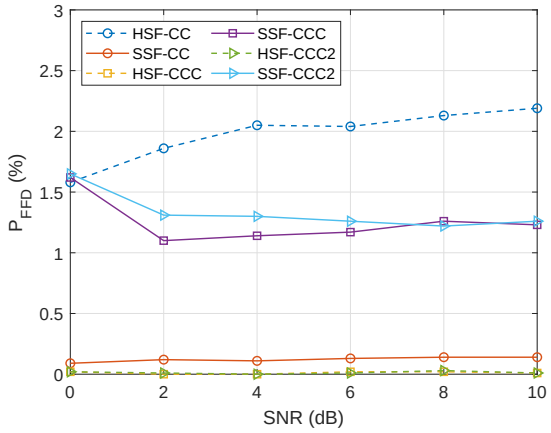

Figure 5: Probability of false failure detection (%) for sensor 2 versus SNR. The passive radar comprises $M = 8$ sensors, with no sensor under failure.

more failed sensors aids in the identification of that damaged, it also increases the rate of sensors rejection and thus of valid measurements, that is the main drawback of the heuristic method.

Figure 7 shows the reaction time of the proposed method in terms of failure detection. Specifically, the figure contains the probability of correct failure detection versus the number of processed samples that range from 10 to 1000.

As expected, the P_{CFD} grows as the number of data increases, but interestingly it can be observed that the proposed SSF-CCC and SSS-CCC2 are capable of ensuring a detection probability equal to 98.4% with only 50 samples. Therefore, confirming the applicability of method also in dynamic environments.

In Figure 8, we show the percentage of sensors classified as under failure under a worse scenario with two faulty sensors. The scenario comprises $M = 6$, $M = 8$, and $M = 10$ sensors, respectively. It can be clearly observed that the case $M = 6$ is the most challenging situation where the proposed SSF-CCC and SSF-CCC2 almost always does not declare two failures; they are capable of detecting only one failure (for the 40% of cases). This result is expected since the presence of two fault sensors over 6 sensors (that corresponds to a 33% of nodes) yields a significant amount of outliers in most of the equations. In such a situation, it is very hard to properly detect the two failures. However, increasing the number of sensors, lead to a situation in which the equation errors are essentially focused on a specific set of equations that could be easily detected and canceled. This is evident in subplot c) whereas the relative frequency for two detected failure is equal to 95%.

In the next numerical examples, we generate a partially-simulated environment where the received signal is acquired through a real system. Specifically, we collect real-recorded data from a WiFi source (IEEE 802.11 standard with 802.11ac only and OFDM packages). The signal is composed of 643 I&Q samples acquired at a carrier frequency of 5.18 GHz, with a sampling frequency of 20 MHz. Starting from this acquisition, the replicas for $M = 8$ sensors are derived by imposing a random delay and adding Gaussian noise in order to rule the specific value of SNR. Results in terms of P_{CFD} are reported in Fig. 9 versus SNR. Interestingly, the curves behaviour follows the trend observed over fully simulated data with the SSF-CCC and SSF-CCC2 returning the maximum performances.

In order to show the benefits of the proposed algorithms on the TDOA estimation, the related RMSE is estimated. The RMSE is computed removing the delay corresponding to each sensor detected as under failure. Additionally, the Cramér-Rao lower bound (CRLB) for delay estimation is also reported. In particular, the considered lower bound is based on the CRLB derived for two sensors in the complex case [19] that is generalized to multiple sensors as in [20], [21]. The corresponding results are shown in Figure 10 as a function of the number of sensors for SNR $= 0$ dB. In addition, the standard CC, CCC, and CCC2 algorithms, summarized in Section II and performing no sensor failure detection, are also considered for comparison purposes. Similarly, the method used before the failure detection process is considered as competitor. In particular, the method is indicated as outlier-cancellation CCC (OC-CCC) and its respective RMSE curves are reported in the same figure.

Subplots a) and b) refer to case in which all sensors are correctly working, whereas subplots c) and d) show the RMSE behavior when sensor number 2 is in failure. As expected subplots a) and b) highlight that all classic methods, viz. CC, CCC, and CCC2, perform better than their counterparts accounting for failure detection. Anyway, the respective losses are quite limited especially for SSF-CCC and SSF-CCC2. On the other hand, subplots c) and d) show that the classic CC/CCC/CCC2 and the OC-CC/CCC/CCC2 methods are not capable of ensuring satisfactory estimation performance when there is at least a sensor in failure. Whereas both SSF-CCC and SSF-CCC2 share good performances with a significant improvement in their RMSE performance also with respect to the HSF-CCC and HSF-CCC2. The curves show that the RMSE reduces as the number of deployed sensors increases

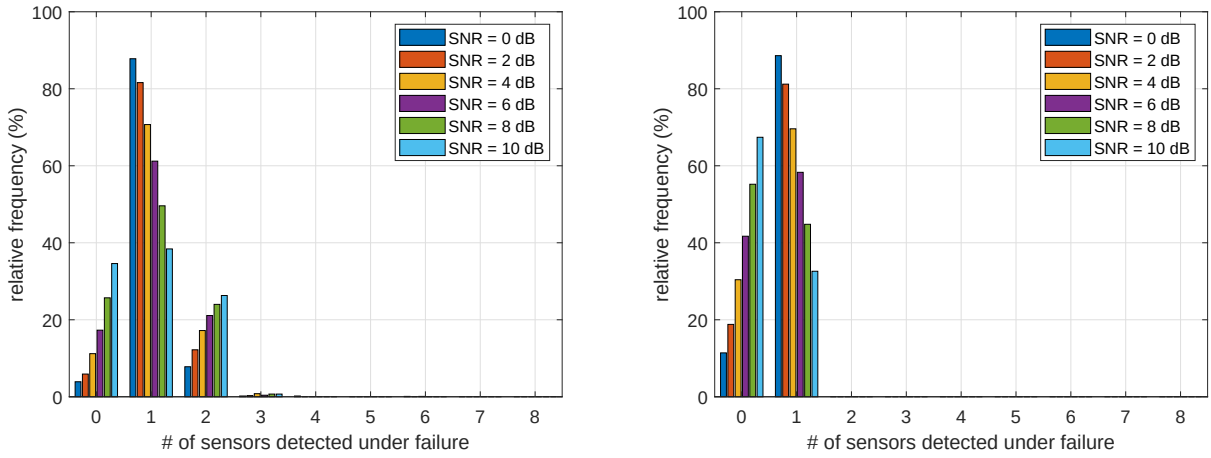

(a) HSF-CC (b) SSF-CC

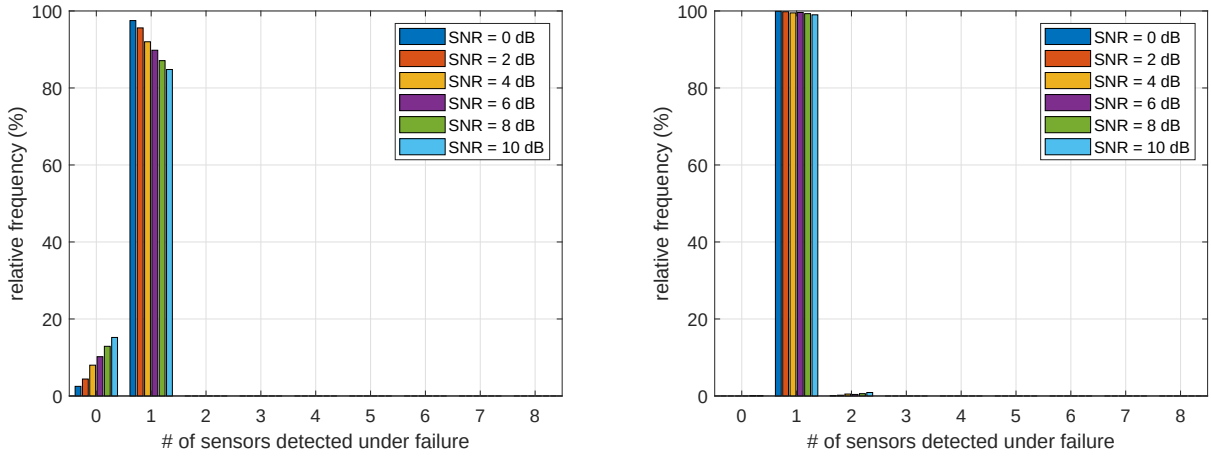

(c) HSF-CCC (d) SSF-CCC

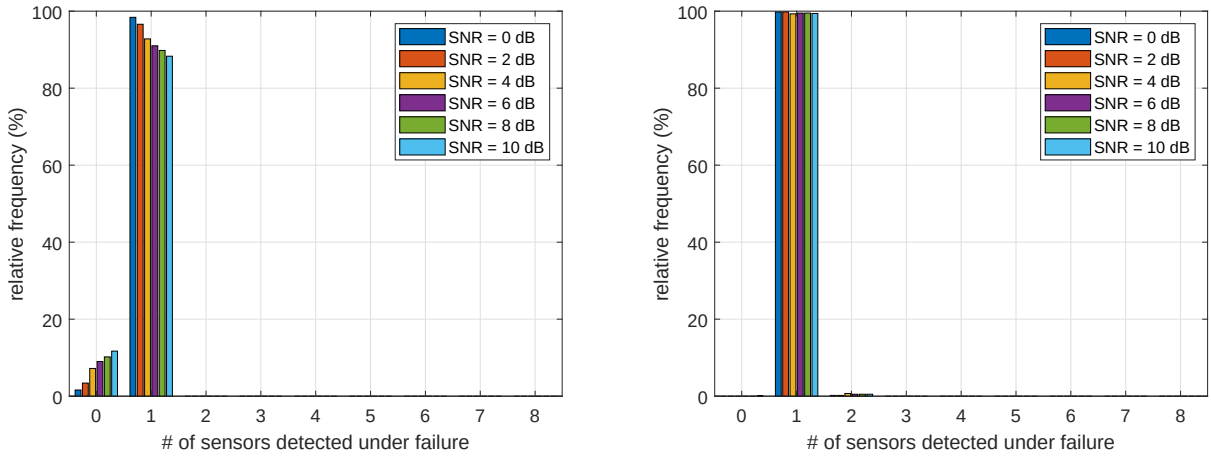

(e) HSF-CCC2 (f) SSF-CCC2

Figure 6: Relative frequency (%) of the number of detected sensors under failure for different SNRs. One sensor is set to be under failure with a number of available sensors for the entire system equal to $M = 8$. A total number of $M_c = 1000$ Monte Carlo simulations are performed. Subplots refer to a) HSF-CC, b) SSF-CC, c) HSF-CCC, d) SSF-CCC, e) HSF-CCC2, and f) SSF-CCC2.

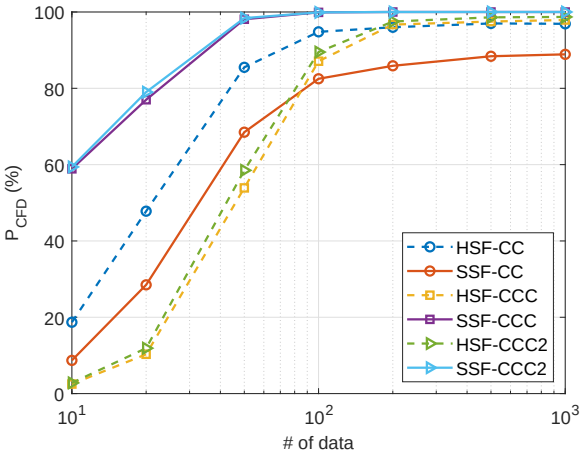

Figure 7: Probability of correct failure detection (%) for sensor 2 versus the number of samples. The passive radar comprises $M = 8$ sensors, with sensor number 2 set to be under failure.

getting closer and closer of the CRLB benchmark. The SSF-CCC2 exhibits the best performance since it uses all possible equations from the correct sensors so better and better refining the delay estimations.

Finally, the study of the impact of the failure detection on the performance of the positioning algorithm is performed using the RMSE of the position estimate as performance metric. More precisely, Figure 11 shows the RMSE of the position for each point in a map of size 500×500 m, considering $M = 7$ sensors located as in the figure. Setting the SNR at the central node, $\text{SNR}_0 = 10$ dB, the SNR values at each node is obtained as [22]:

$$\text{SNR}_i = \text{SNR}_0 \frac{d_0^2}{d_i^2}, \quad i = 1, \ldots, M-1,$$

having indicated with d_0 the distance between the target and the reference node, and with d_i the distance between the target and the i-th receiver.

Subplots in Figure 11 refer to the proposed SSF-CCC, the position estimation performed a priori excluding the fault sensor (indicated as benchmark), and the standard CCC not performing a failure detection. Observing the figures, we see that the proposed SSF-CCC is capable of almost reaching the same performance as the benchmark, whereas the standard CCC completely fails in evaluating the target position. Therefore, it can be claimed that a non-detected sensor under failure is a sufficient condition to completely degrade the localization capabilities of the TDOA-based passive radar.

V. Conclusions

This paper has proposed a novel architecture for delay estimation in TDOA-based passive radars in the presence of outliers and/or sensor failure conditions. Precisely, it is essentially a two-stage architecture that makes use of statistical inferences on the number of outlier equations to declare a sensor failure. In particular, the first stage of the algorithm performs a weak cancellation followed by a strong cancellation of some equations that are identified to be outliers in the devised overdetermined LS problem. Precisely, at each cancellation step, the proposed method computes the MSE of each equation in the system and then rejects those showing an error that is above a preassigned threshold set according to the MAD criterion. Additionally, at the second stage, a failure identification rule based on the statistical behavior of the warning scores has been applied to declare a failure of one or more sensors and discard all their respective measurements. Numerical simulations have proved the effectiveness of the algorithm in identifying and rejecting a defective sensor as well as in properly estimating the delays of signal's replica. Moreover, the robustness of the proposed methods in situations where no sensor is in failure is also demonstrated observing slight losses with respect to the standard method. Possible future research directions could consist in extending the proposed architecture/algorithms to work in environments characterized by multipath as well as in testing the algorithm on real-recorded data.

Acknowledgments

The authors would like to thank the Editor and the anonymous Referees for the interesting questions and comments that have helped us to improve this paper.

The authors wish also to thank Prof. Fabiola Colone and Dr. Francesca Filippini of La Sapienza University of Rome that provided us with real-recorded data.

References

[1] A. Farina and H. Kuschel, "Guest Editorial Special Issue on Passive Radar (Part I)," *IEEE Aerospace and Electronic Systems Magazine*, vol. 27, no. 10, pp. 5–5, 2012.

[2] P. Falcone, F. Colone, A. Macera, and P. Lombardo, "Two-Dimensional Location of Moving Targets within Local Areas using WiFi-Based Multistatic Passive Radar," *IET Radar, Sonar & Navigation*, vol. 8, no. 2, pp. 123–131, 2014.

[3] F. Colone and P. Lombardo, "Polarimetric Passive Coherent Location," *IEEE Transactions on Aerospace and Electronic Systems*, vol. 51, no. 2, pp. 1079–1097, 2015.

[4] H. D. Griffiths and C. J. Baker, *An Introduction to Passive Radar*. Artech House, 2017.

[5] S. Zhang, Z. Huang, X. Feng, J. He, and L. Shi, "Multi-Sensor Passive Localization using Second Difference of Coherent Time Delays with Incomplete Measurements," *IEEE Access*, vol. 7, pp. 43 167–43 178, 2019.

[6] C. Knapp and G. Carter, "The Generalized Correlation Method for Estimation of Time Delay," *IEEE Transactions on Acoustics, Speech, and Signal Processing*, vol. 24, no. 4, pp. 320–327, 1976.

[7] M. Cobos, F. Antonacci, L. Comanducci, and A. Sarti, "Frequency-Sliding Generalized Cross-Correlation: A Sub-Band Time Delay Estimation Approach," *IEEE/ACM Transactions on Audio, Speech, and Language Processing*, vol. 28, pp. 1270–1281, 2020.

[8] L. Pallotta and G. Giunta, "Accurate Delay Estimation for Multi-Sensor Passive Locating Systems Exploiting the Cross-Correlation between Signals Cross-Correlations," *IEEE Transactions on Aerospace and Electronic Systems*, vol. 58, no. 3, pp. 2568–2576, 2022.

[9] J. S. Picard and A. J. Weiss, "Bounds on the Number of Identifiable Outliers in Source Localization by Linear Programming," *IEEE Transactions on Signal Processing*, vol. 58, no. 5, pp. 2884–2895, 2010.

[10] ——, "Time-Delay and Doppler-Shift based Geolocation in the Presence of Outliers," in *2011 4th IEEE International Workshop on Computational Advances in Multi-Sensor Adaptive Processing (CAMSAP)*. IEEE, 2011, pp. 53–56.

[11] ——, "Time Difference Localization in the Presence of Outliers," *Signal Processing*, vol. 92, no. 10, pp. 2432–2443, October 2012.

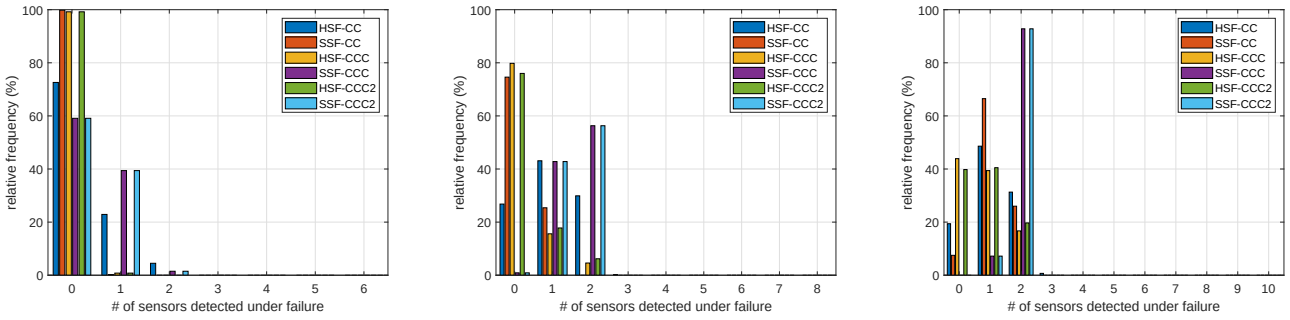

(a) $M = 6$ (b) $M = 8$ (c) $M = 10$

Figure 8: Relative frequency ($\%$) of the number of detected sensors under failure for different SNRs. Two sensors are set to be under failure with the SNR equal to 0 dB. A total number of $M_c = 1000$ Monte Carlo simulations are performed. Subplots refer to a) $M = 6$, b) $M = 8$, and c) $M = 10$.

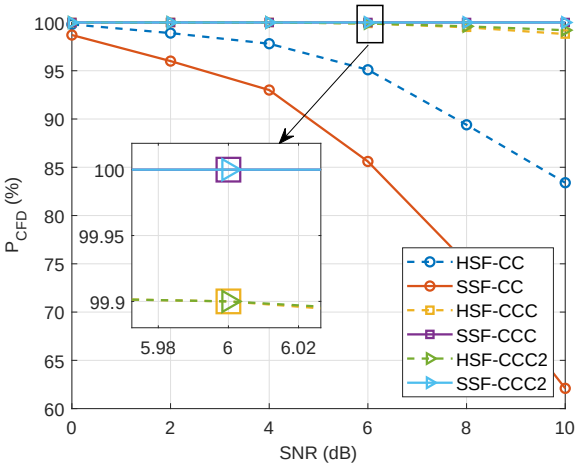

Figure 9: Probability of correct failure detection (%) for sensor 2 versus SNR for real-recorded data. The passive radar comprises $M = 8$ sensors, with sensor number 2 set to be under failure.

[12] I. Enosh and A. J. Weiss, "Outlier Identification for TOA-based Source Localization in the Presence of Noise," *Signal processing*, vol. 102, pp. 85–95, 2014.

[13] N. G. Ferrara, H. Wymeersch, E. S. Lohan, and J. Nurmi, "A Comparison of Bayesian Localization Methods in the Presence of Outliers," in *2017 13th International Wireless Communications and Mobile Computing Conference (IWCMC)*. IEEE, 2017, pp. 1546–1551.

[14] M. Compagnoni, A. Pini, A. Canclini, P. Bestagini, F. Antonacci, S. Tubaro, and A. Sarti, "A Geometrical–Statistical Approach to Outlier Removal for TDOA Measurements," *IEEE Transactions on Signal Processing*, vol. 65, no. 15, pp. 3960–3975, 2017.

[15] C. Leys, C. Ley, O. Klein, P. Bernard, and L. Licata, "Detecting Outliers: Do not use Standard Deviation Around the Mean, use Absolute Deviation Around the Median," *Journal of Experimental Social Psychology*, vol. 49, no. 4, pp. 764 – 766, 2013. [Online]. Available: http://www.sciencedirect.com/science/article/pii/S0022103113000668

[16] H. Fitriyah and A. S. Budi, "Outlier Detection in Object Counting based on Hue and Distance Transform using Median Absolute Deviation (MAD)," in *International Conference on Sustainable Information Engineering and Technology (SIET)*. IEEE, 2019, pp. 217–222.

[17] L. Pallotta, G. Giunta, C. Clemente, and J. J. Soraghan, "SAR Coregistration by Robust Selection of Extended Targets and Iterative Outlier Cancellation," *IEEE Geoscience and Remote Sensing Letters*, vol. 19, pp. 1–5, 2022.

[18] L. Miller and J. Lee, "Error Analysis of Time Delay Estimation using a Finite Integration Time Correlator," *IEEE Transactions on Acoustics, Speech, and Signal Processing*, vol. 29, no. 3, pp. 490–496, 1981.

[19] J. P. Delmas and Y. Meurisse, "On the Cramer Rao Bound and Maximum Likelihood in Passive Time Delay Estimation for Complex Signals," in *2012 IEEE International Conference on Acoustics, Speech and Signal Processing (ICASSP)*, 2012, pp. 3541–3544.

[20] P. Schultheiss, "Locating a Passive Source with Array Measurements: a Summary of Results," in *IEEE International Conference on Acoustics, Speech, and Signal Processing (ICASSP)*, vol. 4. IEEE, 1979, pp. 967–970.

[21] A. Quazi, "An Overview on the Time Delay Estimate in Active and Passive Systems for Target Localization," *IEEE Transactions on Acoustics, Speech, and Signal Processing*, vol. 29, no. 3, pp. 527–533, 1981.

[22] M. A. Richards, J. Scheer, W. A. Holm, and W. L. Melvin, *Principles of Modern Radar*. Citeseer, 2010, vol. 1.

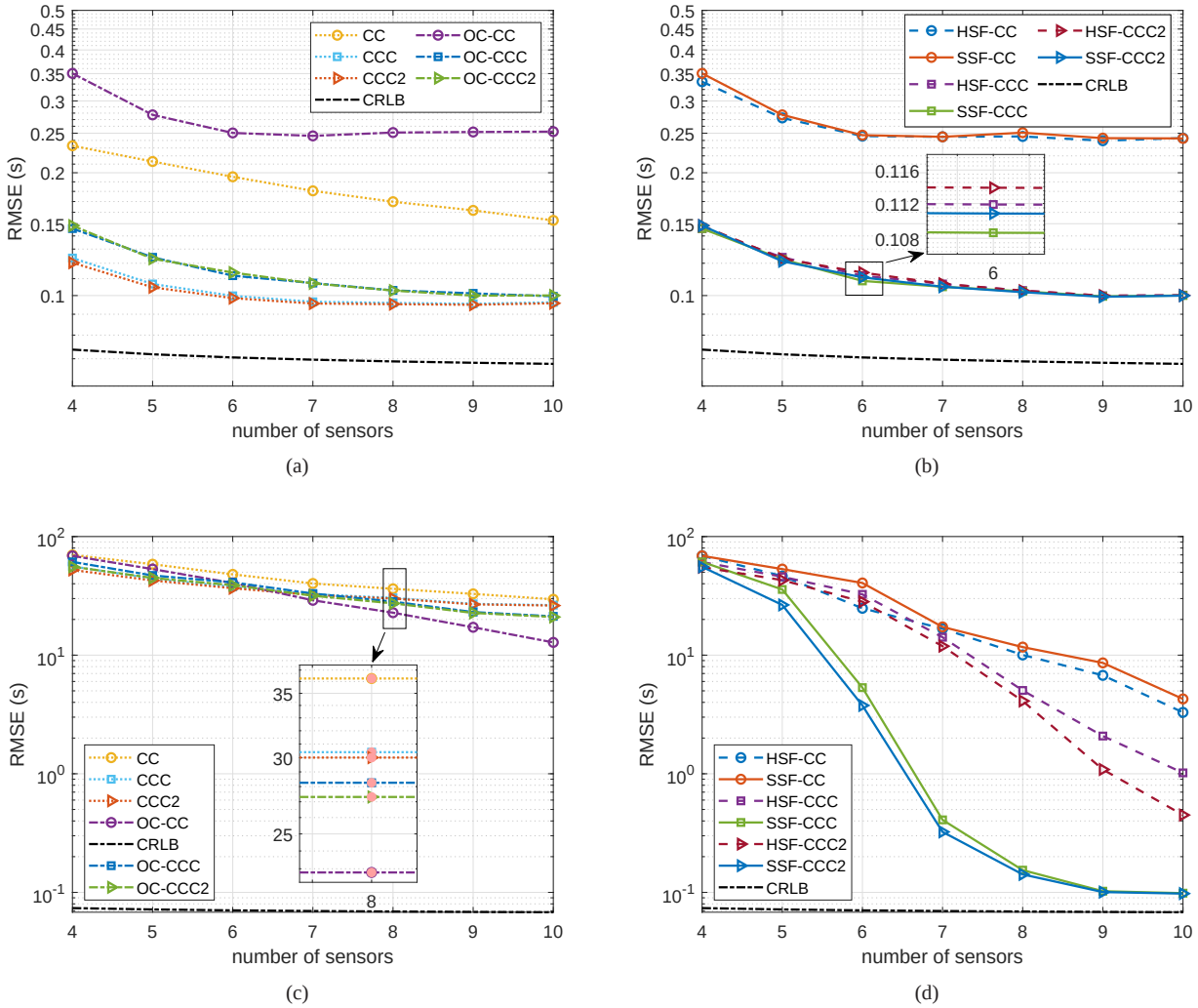

Figure 10: RMSE (s) of the delay estimate versus number of passive receiving sensors M under $H_{F,0}$ (top) and $H_{F,1}$ (bottom) hypotheses. Subplots on left and right refer to the different considered algorithms.

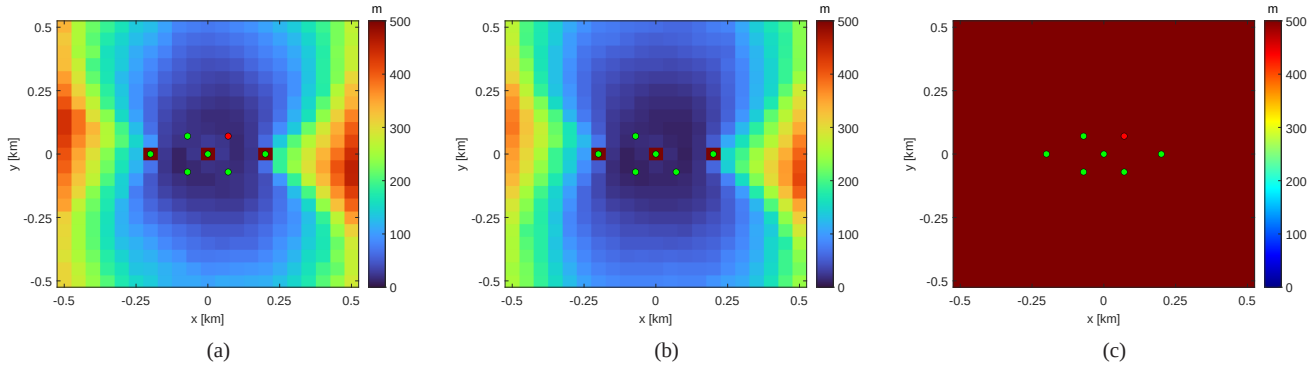

Figure 11: RMSE (m) of the estimated position for $M = 7$ sensors with one under failure. Subplots refer to a) SSF-CCC, b) benchmark for $M = 6$ sensors, and c) CCC. .